Breakup measurements of particle unbound states in ^{10}B

P. J. Leask, M. Freer, N. M. Clarke, B. R. Fulton, C. D. Freeman, and S. M. Singer
School of Physics and Astronomy, University of Birmingham, Edgbaston, Birmingham B15 2TT, United Kingdom

W. N. Catford, N. Curtis, and K. L. Jones
Department of Physics, University of Surrey, Guildford, Surrey GU2 5XH, United Kingdom

R. L. Cowin and D. L. Watson
Department of Physics, University of York, York Y01 5DD, United Kingdom

R. P. Ward
School of Sciences, Staffordshire University, College Road, Stoke-on-Trent ST4 2DE, United Kingdom

N. A. Orr
Laboratoire de Physique Corpusculaire, ISMRA and Université de Caen, IN2P3-CNRS, F-14050 Caen Cedex, France

V. F. E. Pucknell
EPSRC Daresbury Laboratory, Daresbury, Warrington WA4 4AD, United Kingdom
(Received 30 May 2000; published 12 February 2001)

The breakup of ^{10}B has been studied using the ^{7}Li(^{12}C,^{10}B*)^{9}Be two-nucleon transfer reaction with a 76-MeV ^{12}C beam incident on a Li_2O target. The ^{10}B excited states were observed to break up into $\alpha + {}^{6}$Li, $\alpha + {}^{6}$Li(3^+), ^{8}Be$+d$, and ^{9}Be$+p$. Evidence is found for two new states in ^{10}B at excitation energies of 7.96 ± 0.07 MeV and 9.58 ± 0.06 MeV that decay strongly into the $\alpha + {}^{6}$Li(3^+) final state.

DOI: 10.1103/PhysRevC.63.034307 PACS number(s): 27.20.+n

I. INTRODUCTION

The structure of light nuclei has received renewed attention in the light of advances in the study of the properties of exotic, neutron-rich, nuclei. As an example, the prediction that nuclei composed of α particles and valence neutrons and protons can be identified with molecular-type structures analogous to their atomic counterparts has led to a reexamination of the spectroscopic properties of these systems [1–6]. It is suggested that the excited states of ^{10}Be located at ~ 6 MeV may be linked to an $\alpha + 2n + \alpha$ cluster structure in which the two-centered potential formed by the two α-clusters gives rise to molecularlike wave functions for the two neutrons. There should be isobaric analogs of such $T = 1$ states in the nuclei ^{10}B and ^{10}C. In the latter case the spectroscopy is largely unknown, while for ^{10}B it is possible to identify suitable molecular counterparts [1–3]. One important signature of the existence of such states would be their decay properties. For example, the breakup of molecular states in ^{10}Be and ^{12}Be into helium clusters has been used to selectively observe such states [7,8]. Similarly, the decay of states in ^{10}B to particular mass partitions, e.g., $\alpha + {}^{6}$Li(g.s.), ^{8}Be$+d$, ^{9}Be$+p$, and ^{6}Li(0^+:3.56 MeV)$+\alpha$ may also provide evidence for new types of cluster structures in this nucleus with either $T = 1$ or $T = 0$ character.

Here, we present measurements of the breakup of ^{10}B excited states, populated in the ^{7}Li(^{12}C, ^{10}B*)^{9}Be reaction, in which we find evidence for two new $T = 0$ states in ^{10}B, which decay into the final state ^{6}Li(3^+_1)$+\alpha$.

II. EXPERIMENTAL DETAILS

A study of the ^{7}Li(^{12}C,^{10}B*)^{9}Be reaction was performed at the 14UD tandem accelerator facility at the Australian National University. A 76-MeV ^{12}C beam was incident on a 100-μg cm^{-2} Li_2O (on a 10-μg cm^{-2} carbon backing) target foil. The total integrated beam charge was 1.13 mC. The breakup of ^{10}B into the final-state particles $p + {}^{9}$Be, $d + {}^{8}$Be, $d + \alpha + \alpha$, and $\alpha + {}^{6}$Li was observed using an array of four silicon-strip detectors situated on one side of the beam axis in a close-packed geometry. The ^{9}Be recoil particles were detected in coincidence with the breakup products in an array of nine charged-particle telescope detectors (MEGHA [9]) on the opposing side of the beam axis. The ΔE component of the telescopes was a gas ionization chamber with 3.5-μm Mylar windows containing isobutane gas at a pressure of 60 Torr. A two-dimensional position-sensitive silicon detector (active area 5 cm$\times$5 cm) was placed inside the gas volume, and at approximately 5 cm from the window. The silicon detector provided a measure of the residual energy of the incident ions. Details of the operation and performance of these detectors may be found in Refs. [9,10]. The nine hybrid telescopes thus provided a measurement of the charge, energy, and emission angle of each recoil particle. The hybrid telescopes were arranged in a 3×3 square and spanned the polar angular range of 12°–30°. The four strip detectors were placed on the opposite side of the beam axis spanning the polar angular interval of 20°–50°. The azimuthal angles of the hybrid telescopes and the strip detectors were arranged so that it was possible to simultaneously detect all of the particles produced in the above reactions.

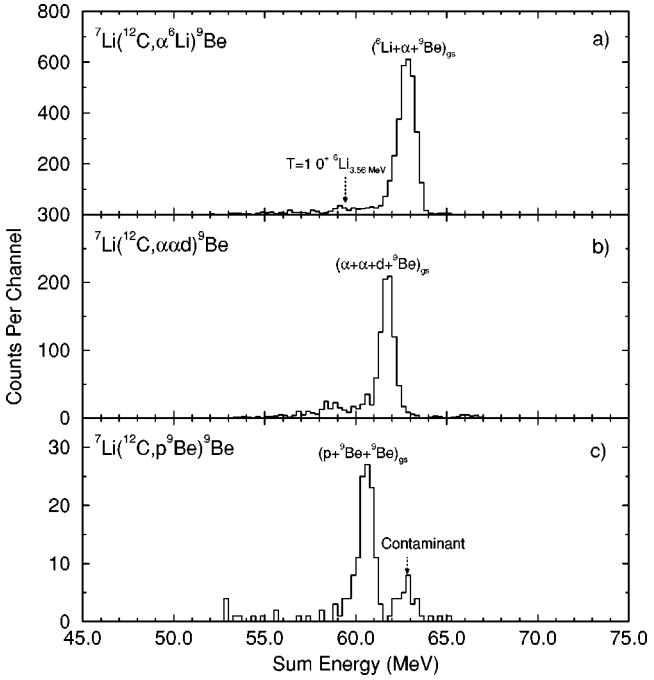

FIG. 1. The sum energy spectra for the reactions (a) ^{7}Li(^{12}C,$\alpha+{}^6$Li)^{9}Be, (b) ^{7}Li(^{12}C,$\alpha+\alpha+d$)^{9}Be, and (c) ^{7}Li(^{12}C,^{9}Be+p)^{9}Be.

This overdetermination of the reaction kinematics was necessary as the strip detectors did not provide any explicit particle identification information. However, the strip detectors possessed 16 position-sensitive strips [10] (oriented horizontally, i.e., toward the beam axis), and thus were able to provide a measurement of the energy and angle of all detected particles. With a combination of this information and that from the hybrid detector telescopes it was possible to reconstruct unambiguously all of the final states of interest. The energy resolution of the strip detectors and telescopes were 200 and 350 keV with corresponding position resolutions of 0.2 and 0.9 mm (at 150 and 600 mm from the target). The detector position and energy responses were calibrated using an α-source and elastic scattering measurements.

III. RESULTS

It is possible to reconstruct the reaction Q values for the reaction ^{7}Li(^{12}C, ^{10}B*)^{9}Be by calculating the difference between the energies for the final-state particles and that of the beam. However, many of the reactions of interest have very similar Q values, and hence are not separated. For example, the Q values for the reactions ^{7}Li(^{12}C,$p+{}^9$Be)^{9}Be, ^{7}Li(^{12}C,$d+{}^8$Be)^{9}Be, and ^{7}Li(^{12}C,$\alpha+{}^6$Li)^{9}Be are -15.08, -14.51, and -12.95 MeV, respectively. Although the energy resolution is sufficient to resolve the α-decay channel, it may not be used to distinguish between the proton and deuteron decays, or even the many other reactions that occur. Thus, the final states were resolved by comparing the momentum of the detected recoil and that of the breakup products. However, as no mass information was available for the particles detected in the strip detectors, it was necessary

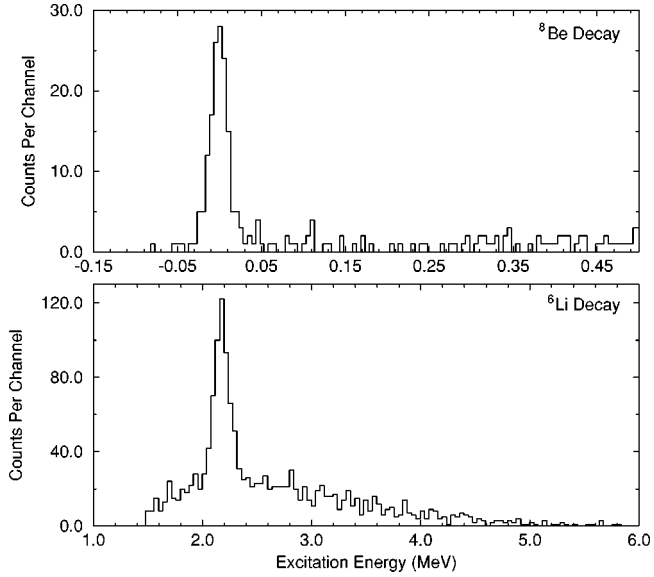

FIG. 2. The reconstructed ^{8}Be (top) and ^{6}Li (bottom) excitation energy spectra for $\alpha+\alpha+d$ coincidences. The two α decay of the ^{8}Be ground state and $\alpha+d$ decay of the 2.186-MeV ^{6}Li state can clearly be identified.

to assume their masses before performing the momentum comparison. By computing the momentum difference for every permutation of particles in a single event, it was possible to identify the mass of each and thus the decay channel. Figure 1 shows the sum of energy spectra (sum of the energies of the final-state particles) for the ^{7}Li target gated on the various final states. It is clear that this procedure has been successful as the peaks lie within 300 keV of their expected values. The only evidence for feed-through of data from one reaction channel to another is for the $\alpha+{}^6$Li decay that produces a small contaminant peak in the $p+{}^9$Be spectrum. In Fig. 1(b) there is evidence for the excitation of the 3.05-MeV $5/2^+$ state in the ^{9}Be recoil. In addition, there is a suggestion of a small peak in Fig. 1(a) in the ^{6}Li+α coincidence spectrum that may be associated with the $T=1$, 0^+, 3.56-MeV state in the ^{6}Li breakup component.

The final state of $\alpha+\alpha+d$ can be arrived at by two different decay paths, either d decay leading to ^{8}Be which in turn decays into two α particles, or ^{10}B decays by α emission to an α-decaying state in ^{6}Li. In either instance, as the masses of the breakup products have been identified, it is possible to reconstruct the excitation energy of the various possible decaying systems. Figure 2 shows the reconstructed excitation energy for ^{8}Be and ^{6}Li. The decays of the ^{8}Be ground state and ^{6}Li 2.186-MeV, $T=0$, 3^+ state can clearly be observed thus enabling the two decay paths to be discriminated.

Figure 3 shows the ^{10}B excitation energy spectra associated with the various decay channels. These have been produced for final states in which all of the particles appear in their ground states. The solid line in these figures is the calculated detection efficiency. This has been calculated using primary angular distributions for the reaction ^{7}Li(^{12}C, ^{10}B*) generated assuming an exponential falloff, and isotropic emission for the decay process. The detection process is then

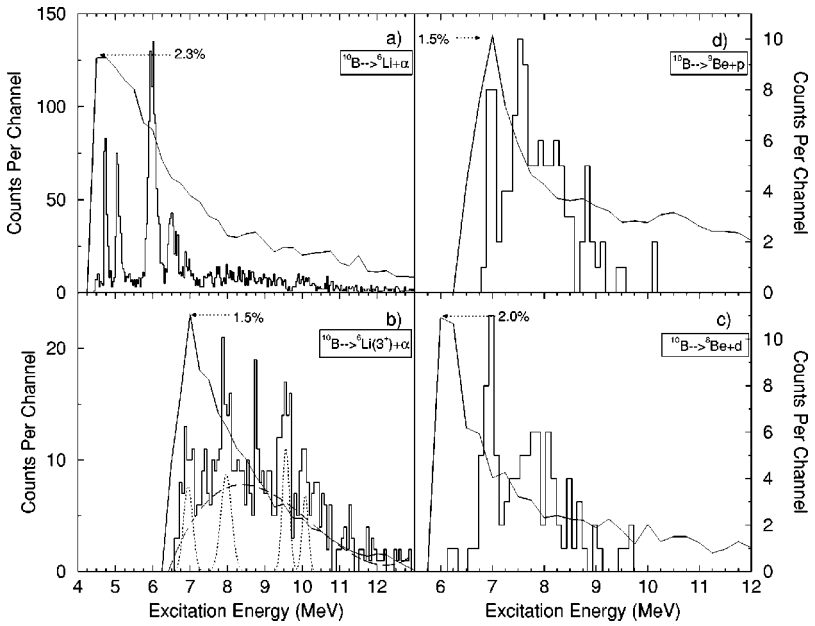

FIG. 3. The ^{10}B excitation spectra for the (a) $\alpha+{}^{6}$Li, (b) $\alpha+{}^{6}$Li(3^{+}), (c) ^{8}Be$+d$, and (d) ^{9}Be$+p$ decay channels. The detection efficiency is shown by the solid line in each instance. In the case of the $\alpha+{}^{6}$Li(3^{+}) channel the dotted lines indicate calculated fits to the peaks observed in the spectrum after subtraction of the background shown by the dashed line.

simulated using the known angular and energy acceptances of the detectors. Although the primary angular distributions are unknown and thus cannot be correctly accounted for in these calculations, as the various reaction channels sample the same center-of-mass angular range for the primary reaction the detection efficiencies may be used to compare the yields in the differing decay channels.

There are a number of states in ^{10}B that have been populated in the two reactions that decay to the various observed final states. Most striking are the decays to the $\alpha+{}^{6}\mathrm{Li}_{\mathrm{g.s.}}$ channel, where the 4.77-MeV (3^{+}) state is clearly observed. The 5.11-MeV (2^{-}) and 5.18-MeV (1^{+}) states are unresolved in the present study, as are the group of states at 5.92 MeV (2^{+}), 6.02 MeV (4^{+}), and 6.13 MeV (3^{-}). An additional peak is observed at 6.54 ± 0.02 MeV, which would correspond to the 6.56-MeV (1^{-}) state. All of these states are known from ^{6}Li$+\alpha$ reactions [11]. A peak at 6.95 ± 0.03 MeV in this decay channel may be associated with both the 6.87-MeV, 1^{-} ($T=0+1$) mixed isospin state and a second state at 7.00 MeV. This peak is observed in the four decay channels identified. The peaks in the ^{8}Be$+d$ and ^{9}Be$+p$ channels lie at 7.02 ± 0.04 and 7.03 ± 0.02 MeV suggesting that it is the latter state that dominates in these spectra. There is also a peak observed in the ^{9}Be$+p$ decay channel [Fig. 3(d)] at 7.62 ± 0.05 MeV that may be associated with either the $T=1$, 7.56-MeV (0^{+}) or 7.67-MeV ($T=0$) state.

There is additional evidence for two states in the ^{6}Li(3^{+})$+\alpha$ decay channel that do not appear in the three other decay channels. The associated peaks [Fig. 3(b)] appear at the excitation energies 7.96 ± 0.07 and 9.58 ± 0.06 MeV (also possibly 10.14 ± 0.08 MeV). These energies have been calculated by fitting Gaussian peaks to the spectrum after subtraction of the background shape shown in the figure. The observation of these levels in only this exit channel indicates that they possess a strong structural link with this final state. The isospin nature of the decay channel also indicates that they possess a $T=0$ character. Although the number of counts associated with each peak is relatively small, the nature of the kinematic reconstruction implies that the spectrum should be clean. The gate on the sum energy peak in Fig. 1(b) selects the $2\alpha+d+{}^{9}\mathrm{Be}_{\mathrm{g.s.}}$ final state. Decays via the ^{6}Li(3^{+}) state are then reconstructed by gating on the 2.186-MeV state shown in Fig. 2. The peak to background ratio in this spectrum is 2.5 to 1, which demonstrates that $\sim$70% of the counts are associated with decays of resonant states in ^{10}B. Thus, it is highly unlikely that the peaks in Fig. 3(b) arise as a result of statistical fluctuations, and that in fact they characterize the decay properties of ^{10}B. This sensitivity is illustrated by the ^{9}Be$+p$ and ^{8}Be$+d$ decay channels, where a peak corresponding to the 6.87-MeV and 7.00-MeV states is clearly identified despite the low statistics.

Table I shows the calculated reaction cross section for

TABLE I. Calculated reaction cross sections for the various breakup channels observed in the ^{7}Li(^{12}C,^{10}B*)^{9}Be reaction.

Reaction channel	Calculated cross section (μb)	Q value (MeV)
^{7}Li(^{12}C,^{9}Be)^{10}B*$\rightarrow{}^{6}$Li$+\alpha$	19.00 ± 0.10	-12.949
^{7}Li(^{12}C,^{9}Be)^{10}B*$\rightarrow{}^{9}$Be$+p$	0.93 ± 0.26	-15.076
^{7}Li(^{12}C,^{9}Be)^{10}B*$\rightarrow{}^{6}$Li*$+\alpha\rightarrow2\alpha+d$	4.61 ± 1.02	-14.424
^{7}Li(^{12}C,^{9}Be)^{10}B*$\rightarrow{}^{8}$Be$+d\rightarrow2\alpha+d$	0.44 ± 0.13	-14.424

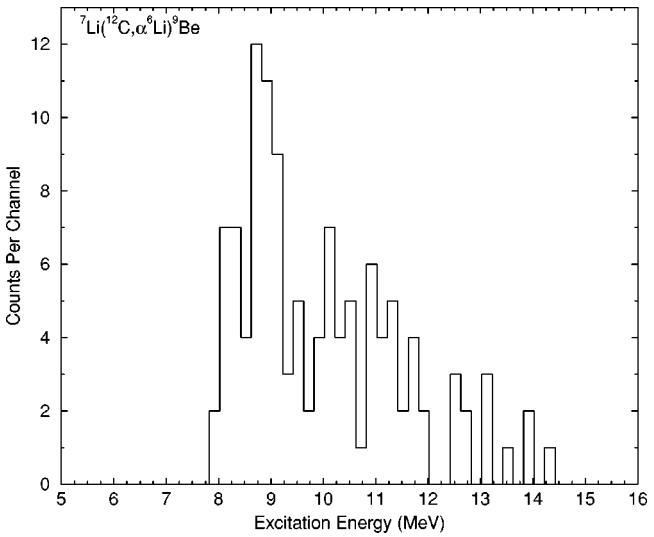

FIG. 4. The ^{10}B excitation spectra for the $\alpha + {}^{6}\mathrm{Li}(0^{+},3.56\ \mathrm{MeV})$ decay channel.

each breakup channel. These values have been evaluated using the following formula:

$$\sigma = \frac{R_t}{N_t n_t \epsilon}, \tag{1}$$

where σ is the cross section for the channel specified, R_t is the total number of detected reaction products, N_t is the number of target nuclei in 100 mm^2 of the target, n_t is the total number of beam particles incident on the target, and ϵ is the experimental detection efficiency. When determining the number of events detected in a particular channel only counts corresponding to excited nuclear states were used, the background events being subtracted from the total number of events. The errors quoted include both the statistical uncertainty as well as the uncertainty in the fitted background shape for each channel. The cross section values indicate that α decay is by far the most dominant decay path. This is to be expected as it has the least negative Q value of any of the processes, implying that the states open to α decay are most strongly populated. The $^{8}\mathrm{Be}+d$, $^{6}\mathrm{Li}^{*}+\alpha$, and $^{9}\mathrm{Be}+p$ breakup channels, which all have similar Q values and populate states in the same excitation energy region, can be used as a measure of the breakup probability to particular final states. These reactions show that α decay is the most likely process followed by proton and then deuteron emission.

Finally, Fig. 4 shows the ^{10}B excitation energy spectrum for decays to the $T=1$ final state $^{6}\mathrm{Li}(0^{+},3.56\ \mathrm{MeV})+\alpha$. Although the number of observed counts is small, there is some evidence for the decay of a state at 8.80 ± 0.16 MeV. This could correspond to either of the $T=1$ states 8.889, 3^{-} or 8.894, 2^{+}. The analog of both of these states have been associated with molecular bands in ^{10}Be [1,2], members of which are believed to decay into $\alpha+{}^{6}$He [7]. Interestingly, as the 0^{+}, 3.56-MeV state is the analog of the ^{6}He ground state, the present decay channel is analogous to the $\alpha + {}^{6}$He decay of ^{10}Be.

For the two-body decay channels the $\alpha+{}^{6}$Li 4.77-MeV peak indicates that the experimental resolution is $\sim$65 keV. These values are consistent with those predicted by the Monte Carlo simulations of the reaction and detection process that include effects such as energy straggling in the target, beam spot size and beam divergence, and the detector position and energy resolutions. For the $\alpha+{}^{6}$Li 4.77-MeV state the calculations predict an excitation energy resolution of 70 keV while in the case of the three-body channel the simulations predict a resolution of 130 keV at an excitation energy of 7.00 MeV.

IV. DISCUSSION

First of all, it is clear that in these measurements the $T=1$ states are not strongly populated, and the ^{10}B excitation energy spectra are dominated by $T=0$ states that decay into $^{6}\mathrm{Li}_{gs}+\alpha$. This is probably related to the relatively small magnitude of the sequential two-nucleon transfer cross section. There is, however, some evidence for $T=1$ states previously observed in this nucleus.

In addition, for the $T=0$, $^{6}\mathrm{Li}(3^{+})+\alpha$ decay channel there is some evidence for new states in ^{10}B. The two peaks observed in the $^{6}\mathrm{Li}(3^{+})+\alpha$ decay channel are difficult to correlate with known states in ^{10}B. Tabulated energy levels

TABLE II. Excitation energies, spins, isospins, widths, and decay modes of ^{10}B states between 7.75 and 10 MeV [11]. Quantities in brackets represent uncertain assignments. The two states marked ''†'' are those observed in the present study. It should be noted that for these levels the deduced widths are upper limits only and include the experimental resolutions.

E_x (MeV)	J^{π}	T	Γ (keV)	Decay mode
7.819	1^{-}		260 ± 30	p
8.07	2^{+}		800 ± 200	γ,p,d
$7.96\pm0.07^{\dagger}$		0	285 ± 91	$\alpha+{}^{6}\mathrm{Li}(3^{+})$
(8.7)	$(1^{+},2^{+})$		($\sim$200)	p
8.889	3^{-}	1	84 ± 7	γ,n,p,α
8.894	2^{+}	1	40 ± 1	γ,p,α
$9.58\pm0.06^{\dagger}$		0	257 ± 64	$\alpha+{}^{6}\mathrm{Li}(3^{+})$
(9.7)		(1)	($\sim$700)	n,p,α
10.84 ± 10	$(2^{+},3^{+},4^{+})$		300 ± 100	γ,n,p

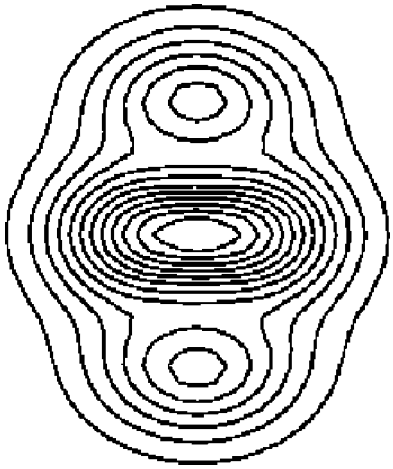

FIG. 5. The density profile of the harmonic oscillator configuration $(n_x,n_y,n_z)=(0,0,0)^4(0,0,1)^2(0,0,2)^4$.

for this nucleus over the energy interval of interest are shown in Table II along with the results from the present study. It is possible to reject all of the previously reported $T=1$ states as candidates for the levels observed in this study due to the isospin of the decay products. Thus the 9.58-MeV peak may be identified as a new $T=0$ state in this nucleus. The measured width of this state is 257 ± 64 keV with the calculated resolution at this excitation energy being 250 keV. Assuming that the peak is composed of just one state then the observed width is clearly dominated by the experimental resolution. The peak at 7.96 MeV lies close to a very broad state reported at 8.07 MeV ($\Gamma=800\pm200$ keV), and is thus unlikely to be connected, and 150 keV higher in energy than the reported 7.819-MeV state. Monte Carlo simulations in this excitation energy region indicate an experimental energy resolution of 190 keV. The measured width of the peak in the spectrum is 285 ± 91 keV, which again indicates that the width is dominated by the experimental resolution. Finally, if the structure at 10.14 MeV is associated with a state then this also has no counterpart in the tabulations for ^{10}B.

This comparison would suggest that nearly all of the peaks in the $^6\mathrm{Li}(3^+)+\alpha$ decay spectrum are new states in ^{10}B previously unobserved because of the strong structural link to the $^6\mathrm{Li}(3^+)+\alpha$ final state. This would imply that such states would not be strongly populated via, for example, the $\alpha+{}^6$Li reaction, and could only be strongly observed in a full kinematic reconstruction of the decay process, such as in the present study. Indeed, inelastic scattering measurements, $[^6\mathrm{Li}(\alpha,\alpha')^6\mathrm{Li}(2.19\ \mathrm{MeV})]$, over the excitation-energy range 10–12 MeV are featureless [12].

The preferred decay path of these states may indicate that they are associated with a $4p$-$4h$ excitation of ^{10}B, with the α particle residing in the s-d shell. The ^{6}Li cluster component would possess a configuration in which the valence $p_{3/2}$ neutron and proton are coupled to $J^\pi=3^+$. The relatively high energy of these states makes it unlikely that the constituents of the α particle would reside in the $p_{3/2}$ level. Furthermore, such a configuration is closely related to that of the ^{10}B ground state, $J^\pi=3^+$. In ^{12}C, for example, a $4p$-$4h$ excitation to the s-d shell results in the 7.65-MeV (0^+) state, which is close in energy to the present states [13]. Indeed, the ^{12}C ground state is believed to possess a $\sim10\%$ contribution from $4p$-$4h$ configurations [13], which could facilitate the population of the proposed states in ^{10}B.

Using the ideas developed in [14], it is possible to gain some insight into the possible nuclear structure associated with such a configuration using harmonic oscillator wave-functions. Figure 5 shows the density that would correspond to the HO configuration $(n_x,n_y,n_z)=(0,0,0)^4(0,0,1)^2(0,0,2)^4$, i.e., in the shell model limit four particles in the $1s_{1/2}$ level, two particles in the $1p_{3/2}$ orbit, and the last four particles in the $d_{5/2}$ orbit that is energetically favored in a prolate-deformed potential (i.e., the [200]1/2 Nilsson orbit). Here, the individual α particles lose their identity, with a region of high density at the center of the plot. However, the configuration does possess two diffuse regions that would then closely correspond to the locus of the unpaired neutron and proton in the $1p_{3/2}$ orbit. Such a structure may be a close analog of the molecular types of configurations that have been suggested for ^{10}Be [1–6].

ACKNOWLEDGMENTS

The authors would like to acknowledge the assistance of ANU personnel in running the accelerator. This work was carried out under a formal agreement between the U.K. Engineering and Physical Sciences Research Council and the Australian National University. P.J.L., C.D.F., and K.L.J. would like to acknowledge the EPSRC for financial support.

[1] W. von Oertzen, Z. Phys. A **354**, 37 (1996).
[2] W. von Oertzen, Z. Phys. A **357**, 355 (1997).
[3] W. von Oertzen, Nuovo Cimento **110**, 895 (1997).
[4] Y. Kanada-En'yo, H. Horiuchi, and A. Doté, Phys. Rev. C **60**, 064304 (1999).
[5] S. Okabe and Y. Abe, Prog. Theor. Phys. **61**, 1049 (1971).
[6] M. Seya, M. Kohno, and S. Nagata, Prog. Theor. Phys. **65**, 204 (1981).
[7] N. Soić *et al.*, Europhys. Lett. **34**, 7 (1996).
[8] M. Freer *et al.*, Phys. Rev. Lett. **82**, 1383 (1999).
[9] R.L. Cowin *et al.*, Nucl. Instrum. Methods Phys. Res. A **423**, 75 (1999).
[10] N. Curtis *et al.*, Nucl. Instrum. Methods Phys. Res. A **351**, 359 (1994).
[11] F. Ajzenberg-Selove, Nucl. Phys. **A490**, 1 (1988).
[12] H.R. Blieden, G.M. Temmer, and K.L. Walsh, Nucl. Phys. **49**, 209 (1963).
[13] N. Takigawa and A. Arima, Nucl. Phys. **A168**, 593 (1971).
[14] M. Freer, R.R. Betts, and A.H. Wuosmaa, Nucl. Phys. **A587**, 36 (1995).